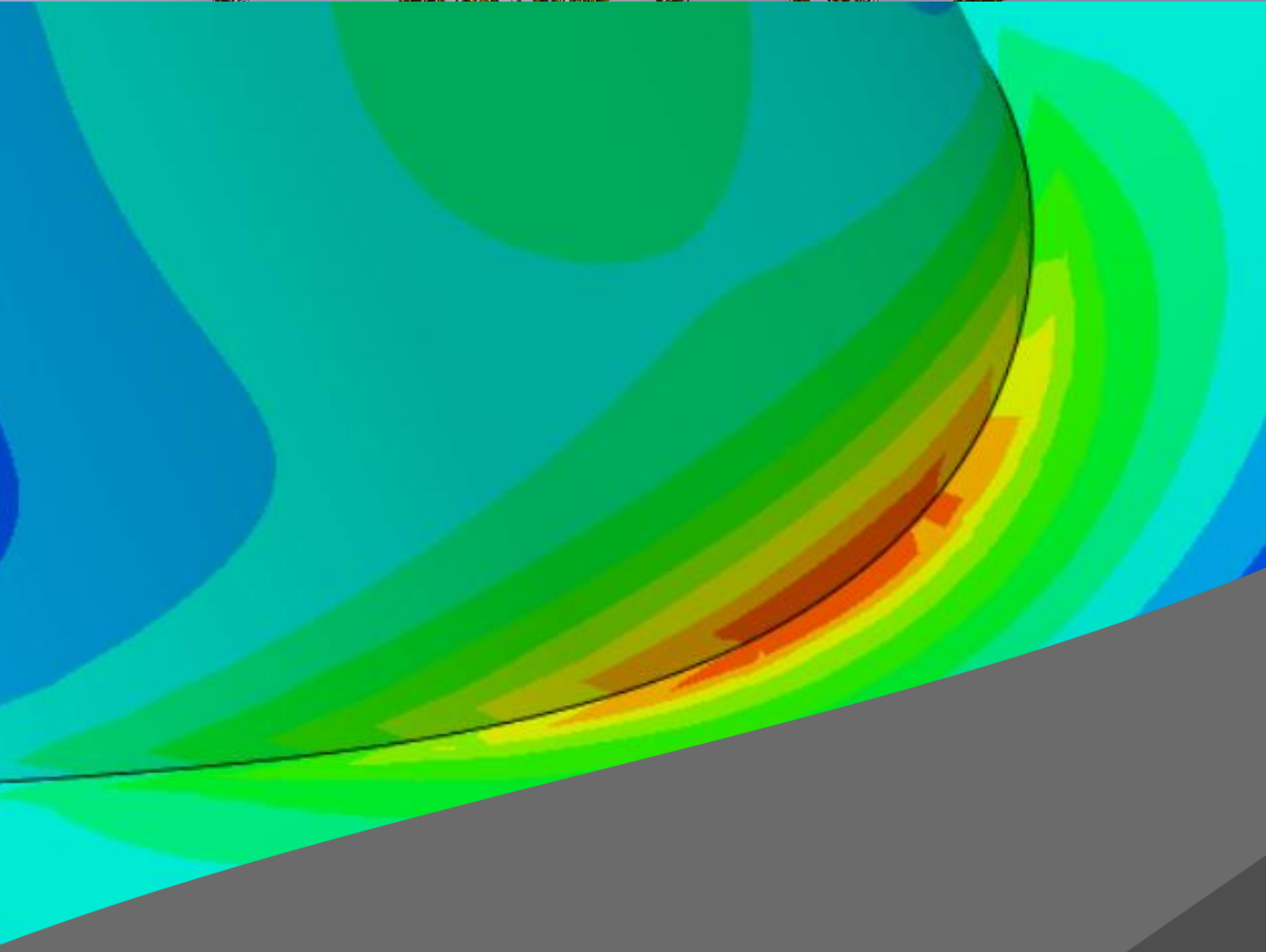


Stress Concentration Factors in Tubular X-Joints

Author: Ruben Schuurman
Date: 17-06-2025

TU Delft

Stress Concentration Factors in Tubular X-Joints

by

Ruben Schuurman

In partial fulfilment of the requirements for the degree of:

Bachelor of Science
in Civil Engineering

at Delft University of Technology,
to be defended publicly on Wednesday June 25, 2025 at 3:10 PM.

Student number:	5638852	
Project duration:	April 22, 2025 – June 23, 2025	
Thesis committee:	Prof. dr. M. Veljkovic,	TU Delft, supervisor
	Dr. ir. P.C.J. Hoogenboom,	TU Delft, examiner
	Ir. H. El Bamby,	TU Delft, supervisor

TU Delft

Preface

In front of you lies my bachelor's thesis, "Stress Concentration Factors in Tubular X-Joints". This thesis has been written to complete my bachelor's degree in Civil Engineering at Delft University of Technology. It is one of the final components required to obtain my degree. Besides this thesis, I am also still working on the courses Numerical Mathematics and System Dynamics. I have been researching and writing on this topic from April to June 2025.

Carrying out this research was a completely new step for me. During the bachelor's program, I gained some experience with writing and literature research, but I had never worked on investigating a completely new topic. This made working on this research refreshing but also challenging. In addition, it turned out not to be easy to combine this with two other courses, but I have managed to complete it. I am proud of the result.

I would like to thank my supervisors, Prof. dr. Milan Veljkovic and Hagar El Bamby, for helping me during this process. I would also like to thank dr. ir. Pierre Hoogenboom for stepping in as an additional examiner. I am grateful for the feedback and insights, and for making it possible for me to complete this thesis. Thanks should also go to TU Delft for the facilities it provides me as a student, such as access to literature databases and the necessary software. Lastly, special thanks to my family and girlfriend for supporting me.

Delft, June 2025
Ruben Schuurman

Abstract

This bachelor thesis investigates how geometric parameters and the type of weld connection influence the stress concentration factors (SCF) in steel X-joints consisting of circular hollow sections (CHS). Such connections are widely used in structures such as trusses, bridges and offshore platforms, where fatigue behaviour is of great importance. The research focuses on the effect of the chord slenderness ratio γ, brace-to-chord thickness ratio τ, and butt and fillet welds. Using finite element analysis (FEA) in Abaqus 2023, 20 models were analysed: 10 with butt welds and 10 with fillet welds. The hot-spot stress method was applied to determine the SCFs at the crown and saddle locations within the modelled joints. The results show that SCFs increase with higher γ and τ, especially in the saddle region of the connection. It also shows that adding fillet welds results in significantly lower SCFs than when using butt welds. The maximum SCF is approximately 30% lower with fillet welds, despite the assumption of a 1 mm root gap between the brace members and chord.

The results largely coincide with the empirical formulas from DNV-RP-C203 for butt welds but differ for fillet welds. This shows that these existing guidelines do not sufficiently consider the weld shape. Limitations of this study include the sole focus on 90° connections and the use of CHS. Only static axial loading was considered and only a limited number of models were analysed due to time constraints.

Future research is recommended to expand the number of models, investigate variations in weld length and weld quality (without or with larger root gap), and analyse connections with different angles. With a more extensive data set, empirical formulas can be derived that better reflect practice. This study contributes to a better understanding of stress concentration in tubular joints and shows how a more optimized joint design can lead to more durable and material-efficient structures.

Table of Contents

List of Tables and Figures **xi**

1 Introduction **1**

2 Theory **2**
2.1 Stress Concentration Factors 2
2.2 X-Joint Geometry and Parameters 2
2.3 SCF Calculation Based on DNV Guidelines 3

3 Methodology **6**
3.1 Finite Element Modelling 6
3.2 Parametric Study 9
3.3 SCF Calculation Using the Hot-Spot Stress Method 10

4 Results **11**

5 Discussion **15**

6 Conclusions and Recommendations **17**

References **19**

List of Tables and Figures

Table 1 Geometric parameters of the baseline model 6
Table 2 Material properties of steel used for the model 7
Table 3 Model variations used for the parametric study 9
Table 4 Extrapolation points, as proposed in DNV-RP-C203 (DNV, 2021) 10
Table 5 Stress concentration factors for the butt-welded joint 11
Table 6 Stress concentration factors for the fillet-welded joint 13

Figure 1. Illustration of a X-joint (DNV, 2021). 3
Figure 2. Influence of the joint geometry on SCFs, using the empirical equations from the DNV guide. 4
Figure 3. Reduction factors F1 and F2, using the equations from the DNV guide. 5
Figure 4. Baseline model of the butt-welded joint, as modelled in Abaqus. 7
Figure 5. Baseline model of the fillet-welded joint, as modelled in Abaqus. 8
Figure 6. Fillet weld root gap, as modelled in Abaqus. Left: cross-section view at the saddle of the joint; right: fillet weld hidden, highlighting the root gap. 8
Figure 7. Meshed fillet-welded model for T = 20 mm. Left: overview of the meshed model; right: detailed view of the meshed fillet weld. 9
Figure 8. Left: extrapolation points (Zavvar et al., 2025); right: geometric parameters DNV-RP-C203 (DNV, 2021). 10
Figure 9. Plot of the stress concentration factors against the chord slenderness γ, for the butt-welded joint 11
Figure 10. Maximum principal stresses in the butt-welded joint with baseline geometry. Upper left: stresses masked on the undeformed model; upper right: stresses masked on the deformed model; bottom left: stresses in the connection at the saddle; bottom right: stresses in the connection at the crown. 12
Figure 11. Plot of the stress concentration factors against the chord slenderness γ, for the fillet-welded joint 13
Figure 12. Maximum principal stresses in the fillet-welded joint with baseline geometry. Upper left: stresses masked on the undeformed model; upper right: stresses masked on the deformed model; bottom left: stresses in the connection at the saddle; bottom right: stresses in the connection at the crown. 14
Figure 13. Comparison between the SCFs of the butt- and fillet-welded joint 15
Figure 14. Comparison between the SCFs as found in this research, and as formulated in the DNV guidelines 16

1 Introduction

This bachelor thesis focuses on the influence of geometric parameters on the stress concentration factors (SCF) in tubular X-joints. A tubular joint is a welded connection between at least two circular hollow steel sections, and are frequently used in structural applications such as trusses, bridges, and offshore platforms.

Stress concentration factors represent the ratio between peak and nominal stresses. Stresses tend to concentrate at points of geometric irregularity. Locally, this causes a significantly higher tension than applied. This behaviour has a big effect on the lifetime performance of a structure, especially its resistance against fatigue. High SCFs can accelerate fatigue failure.

In tubular joints, stresses build up at the welded connection between the brace and chord members. Because of their wide application in (dynamically loaded) structures, understanding how this behaviour works is essential to ensure structural safety.

Innovative technologies, such as 3D printing of steel, offer potential for optimizing joint geometries to minimize SCFs, but their application requires a better understanding of how weld types and geometric parameters influence the stress concentration factors.

This bachelor thesis aims to answer the main research question:

> *How do the geometric parameters and weld type of a tubular X-joint influence the stress concentration factors?*

To answer this question, the study addresses the following sub-questions:

1. *How does the geometry of X-joints influence SCFs according to the DNV code?*

2. *How do chord slenderness γ and brace-to-chord thickness ratio τ affect SCFs based on a finite element model?*

3. *How does the weld type (butt or fillet) affect SCFs?*

This study utilizes finite element analysis (FEA). Using Abaqus 2023, multiple models of joints with circular hollow sections (CHS) are analysed. The research focuses on the effects of γ, τ, and the weld type (butt or fillet) on SCFs. The results are validated against the empirical formulas for SCFs in DNV-RP-C203. The scope is limited to 90° X-joints with CHS, excluding other joint types (e.g., Y-joints) or non-circular sections. Only static axial loads are considered, excluding bending moments or dynamic loading, which are critical for fatigue life but beyond this study's focus. The thesis is structured as follows: Section 2 provides theoretical background, Section 3 details the FEA methodology, Section 4 presents the results, Section 5 discusses the results, and Section 6 offers conclusions and recommendations.

2 Theory

2.1 Stress Concentration Factors

The stress concentration factor (SCF) is the ratio between the peak stress and the nominal stress in an element. In a tubular joint, stresses build up around the connection between the chord and the brace due to a geometric discontinuity. This causes a locally higher stress than the nominal load on the brace. This stress behaviour influences the fatigue resistance of a joint and is therefore of great importance for the structural safety of a construction (Ahmadi et al., 2012; Cao et al., 2018; Kumar et al., 2018)

The formula for the SCF is as follows:

$$\text{SCF} = \frac{\sigma_{peak}}{\sigma_{nom}}$$

where σ_{peak} is the peak stress in the joint, and σ_{nom} is the nominal stress in the brace. Note that the SCF is a dimensionless factor. If a consistent unit is used, the chosen scale does not affect the SCF.

To determine σ_{peak}, the hot-spot stress (HSS) extrapolation method is used. In the remainder of this document, σ_{HS} refers to the peak, or hot-spot, stresses. DNV-RP-C203 (DNV, 2021, p. 22) defines the HSS as "the greatest value of the extrapolation of the maximum principal stress distribution immediately outside the region effected by the geometry of the weld." The method used to compute the HSS is explained in Section 3.3.

For σ_{nom} in the brace, the general equation for stress is used. Since this research exclusively uses circular hollow sections, this can be directly expressed as:

$$\sigma_{nom} = \frac{F}{A} = \frac{F}{\frac{1}{4}\pi\,(d^2 - (d - 2t)^2)}$$

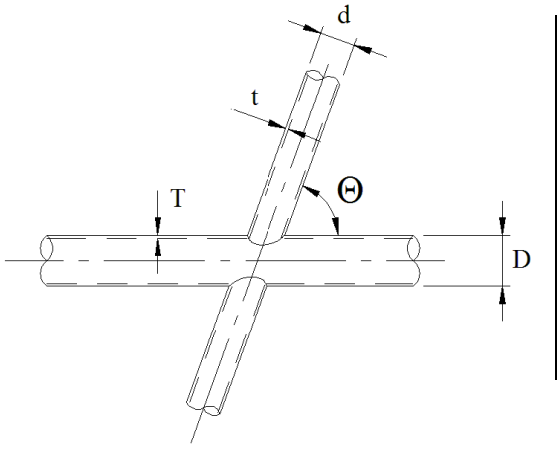
where d is the diameter of the brace and t is the wall thickness of the brace. This formula only applies to axial loads and does not account for in-plane or out-of-plane bending moments.

2.2 X-Joint Geometry and Parameters

Before the effects of the geometric parameters are briefly examined in Section 2.3 using the empirical formulas from DNV-RP-C203 (DNV, 2021), these parameters are first defined. These are also used for creating and analysing the models in Abaqus.

This study is limited to 90° X-joints. Figure 1 shows an illustration of such a connection. The dimensional geometric parameters are indicated in this drawing. Here, d is the diameter in mm of the brace members, D is the diameter in mm of the chord, t is the wall thickness in mm of the brace members, T is the wall thickness in mm of the chord, and θ is the angle in degrees between the chord and brace members measured as in the figure.

In addition to the model dimensions, dimensionless parameters are often used in studies and design guides as well (DNV, 2021; Kumar et al., 2018; NEN, 2025b; Schürmann et al., 2020). These are ratios between the geometry of the connection. The non-dimensional parameters are given below:



Brace-to-chord thickness ratio: $\tau = \frac{t}{T}$

Diameter ratio: $\beta = \frac{d}{D}$

Chord slenderness ratio: $\gamma = \frac{D}{2T}$

Length ratio: $\alpha = \frac{2L}{D}$

Figure 1. Illustration of a X-joint (DNV, 2021).

2.3 SCF Calculation Based on DNV Guidelines

In addition to FEA of tubular X-joints in Abaqus to determine the effects of geometric parameters and weld types on SCFs, the parametric study is also performed using the empirical formulas outlined in Table B2 of Appendix B in DNV-RP-C203 (DNV, 2021).

These equations make it possible to easily determine SCFs using only the joint geometry, making it straightforward to plot the effect of individual parameters on stress concentration. The DNV guide specifies that these equations are only valid within a certain range of parameters, the range of validity of these equations is provided as follows:

$$\begin{aligned} 0.2 \leq\ & \beta\ \leq 1.0 \\ 0.2 \leq\ & \tau\ \leq 1.0 \\ 8 \leq\ & \gamma\ \leq 32 \\ 4 \leq\ & \alpha\ \leq 40 \\ 20° \leq\ & \theta\ \leq 90° \end{aligned}$$

To increase the applicability of the study, also the range of validity specified in NEN-EN 1993-1-8 (NEN, 2025b) was taken into account. The guide specifies that:

$$\frac{D}{T} \leq 40; \qquad \frac{d}{t} \leq 50$$

For X-joints under an axial load the following formulas apply:

Chord saddle: $\mathrm{SCF}_{c,s} = 3.87\gamma\tau\beta(1.10 - \beta^{1.8})(\sin\theta)^{1.7}$

Chord crown: $\mathrm{SCF}_{c,c} = \gamma^{0.2}\tau(2.65 + 5(\beta - 0.65)^2) - 3\tau\beta\sin\theta$

Brace saddle: $\mathrm{SCF}_{b,s} = 1 + 1.9\gamma\tau^{0.5}\beta^{0.9}(1.09 - \beta^{1.7})(\sin\theta)^{2.5}$

Brace crown: $\mathrm{SCF}_{b,c} = 3 + \gamma^{1.2}(0.12\exp(-4\beta) + 0.011\beta^2 - 0.045)$

The DNV guide states that for joints with $\alpha < 12$ the SCF of the saddle can be lowered by a factor F1 for fixed chord ends, or F2 for pinned chord ends. The formulas for these factors are:

$$\mathrm{F1} = 1 - (0.83\beta - 0.56\beta^2 - 0.02)\gamma^{0.23}\exp(-0.21\gamma^{-1.16}\alpha^{2.5})$$
$$\mathrm{F2} = 1 - (1.43\beta - 0.97\beta^2 - 0.03)\gamma^{0.04}\exp(-0.71\gamma^{-1.38}\alpha^{2.5})$$

To visualize graphs of the SCFs for each parameter independently, a set of constant parameters is used. These constant values are the same values that are used for the FEA in Abaqus. Whenever one parameter is varied, the others are kept constant, so a two-dimensional plot can be visualized, clearly highlighting the influence of this individual parameter on the SCFs.

The constant values used are: $\gamma = 9.2$, $\tau = 0.44$, $\beta = 0.6$, and $\alpha = 5.43$ (Schürmann et al., 2020). Staying within the range of validity for each parameter, the graphs in Figure 2 and Figure 3 are illustrated.

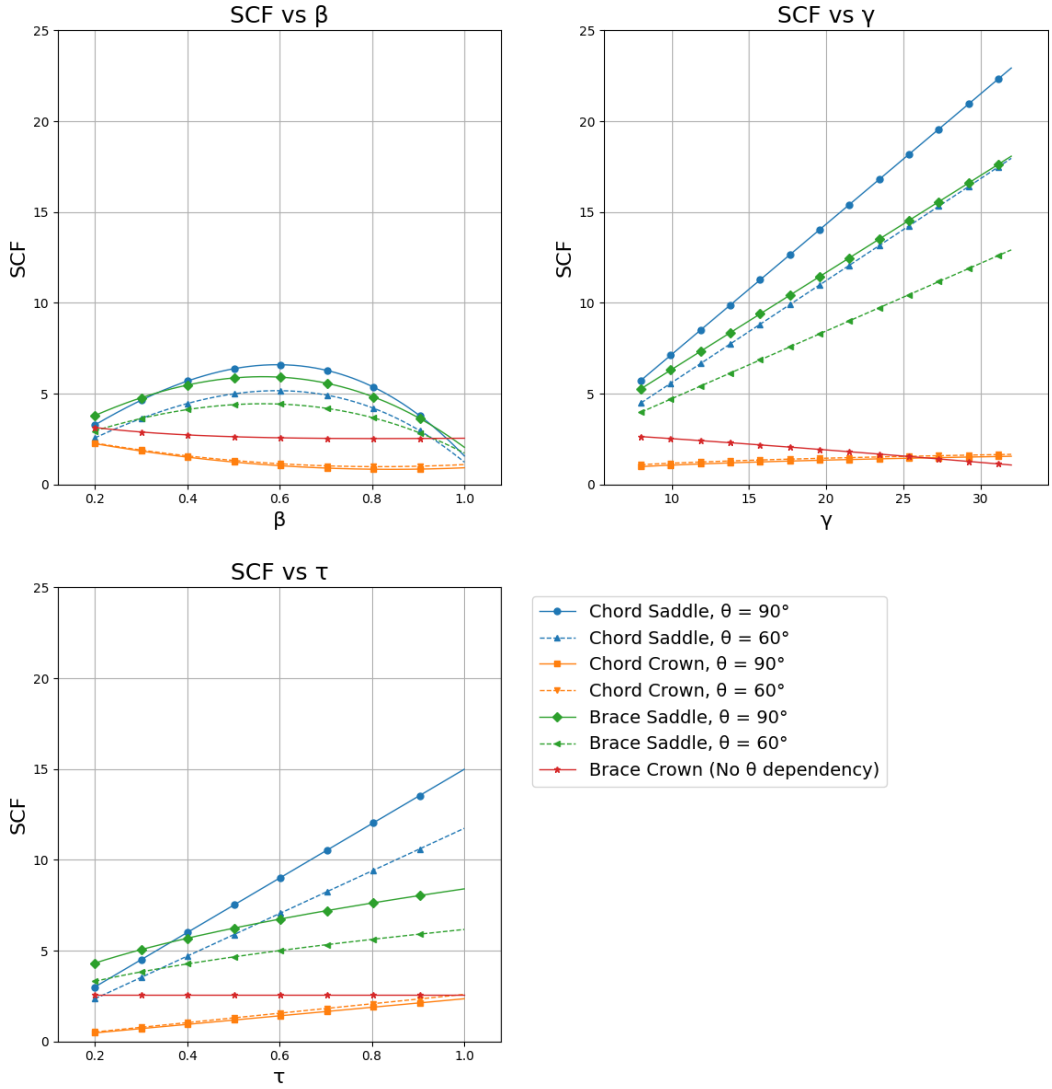


Figure 2. *Influence of the joint geometry on SCFs, using the empirical equations from the DNV guide.*

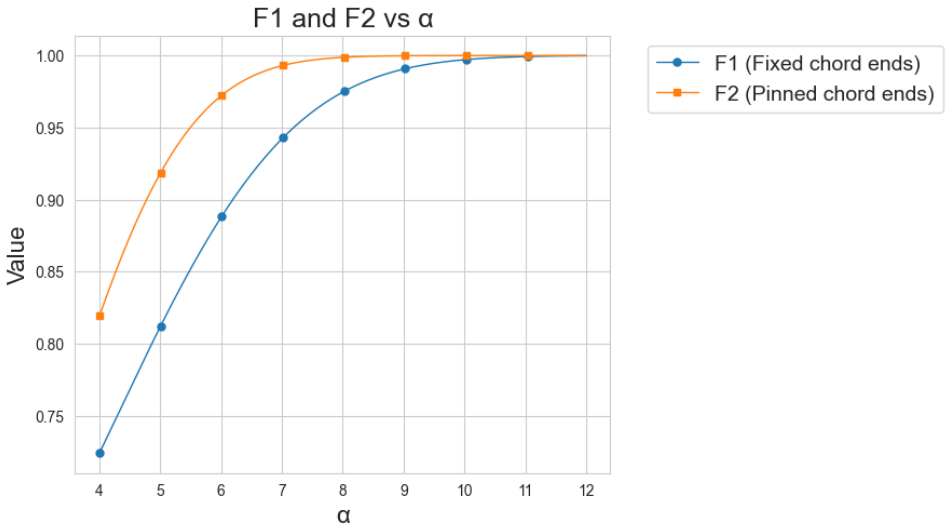


Figure 3. *Reduction factors F1 and F2, using the equations from the DNV guide.*

3 Methodology

The models of the X-joint were created using Abaqus 2023, following the procedure highlighted in Section 3.1. Abaqus is a software package designed for Finite Element Analysis (FEA). In total, 20 models were generated: 10 models of a butt-welded joint and 10 models of a fillet-welded joint, each with a different geometry. Section 3.2 explains how the parametric study was performed. In Abaqus, accurate stress analysis was performed in order to obtain the maximum principal stresses at the crown and saddle locations. From these stresses the SCFs were derived. Section 3.3 describes how this was done.

3.1 Finite Element Modelling

Initially, a baseline model was created, which served as the foundation for the FEA study. The geometry of this model is drawn from Schürmann et al. (2020). Table 1 provides the value for each geometric parameter.

Table 1
Geometric parameters of the baseline model

Parameter[a]		
D	368	mm
T	20	mm
d	220.80	mm
t	8.80	mm
L	1,000	mm
α	5.43	-
β	0.60	-
γ	9.20	-
τ	0.44	-
θ	90°	

[a] *In Schürmann et al. (2020) only the non-dimensional parameters α, β, γ, and τ are given alongside D. The other parameters were derived using the expressions from Section 2.2.*

The baseline model was created by first modelling the chord and brace parts separately, after which they were connected in a three-dimensional assembly. The braces were initially developed using regular circular hollow sections, then portions were cut out to connect them to the chord without intersecting it.

The model was made using homogeneous solid elements. Cao et al. (2018) explained that shell elements could have reduced storage requirements, but the model would not have been able to accurately represent the discontinuous geometry of the joint. In this case, storage space was not a limiting issue. To simulate the behaviour of steel, the material properties listed in Table 2 were assigned to the model. An illustration of the model is shown in Figure 4.

Table 2
Material properties of steel used for the model

Property		
Young's Modulus E	210,000	MPa (N/mm^2)
Poisson's Ratio ν	0.30	-
Density ρ	7.85E-9	tonne/mm^3

Note. The values were taken from NEN-EN 1993-1-1 (NEN, 2025a) and NEN-EN 1991-1-1 (NEN, 2019). For the input in Abaqus, the values were converted from SI to SI-mm units. According to NEN 1991-1-1, the density of steel typically ranges from 7700 to 7850 kg/m^3, the highest value was chosen.

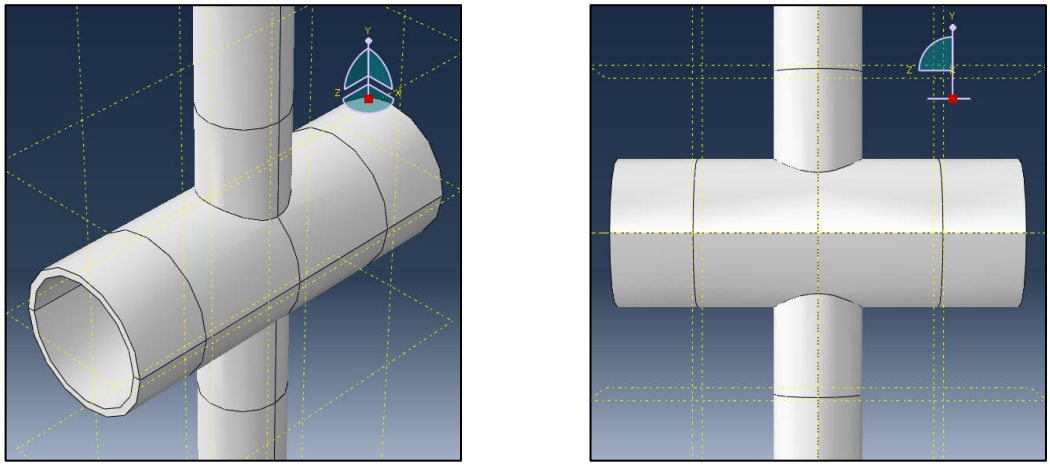


Figure 4. *Baseline model of the butt-welded joint, as modelled in Abaqus.*

To run stress analysis on the joint, the model was subjected to a static axial tensile force of 500,000 N. This force was applied to the upper brace end. To enable the software to solve the problem, boundary conditions were defined. The bottom of the configuration is fully fixed, preventing any displacement or rotation. The top of the joint is only allowed to move vertically, needed for the application of the load.

The model from Figure 4 represents the butt-welded model, where the braces and chord are directly connected through the weld material. A model of the fillet-welded X-joint was also created by duplicating the butt-welded model. To this second model fillet welds were added using a loft path around the brace-to-chord connections. The fillet welds in the model all have a constant leg length of 11.3 mm, leading to a throat thickness of around 8 mm at the crown. An illustration of the fillet-welded model is shown in Figure 5.

When connecting two sections with a fillet weld ideally all the material is connected, but sometimes there remains a small gap at the root of the weld. Meaning the two sections are not fully attached. This introduces a significant discontinuity in the connection. To include this occurrence into the analysis, a small gap of 1 mm thick was left between the braces and chord, see Figure 6.

After both the fillet-welded and butt-welded models were created, additional models were made by copying these. The duplication automatically copied the assembly, assigned properties, applied load, and boundary conditions to each new model. For each of these models, the chord wall thickness T was adjusted using a solid sweep or sweep cut, resulting in 10 variations for each weld type.

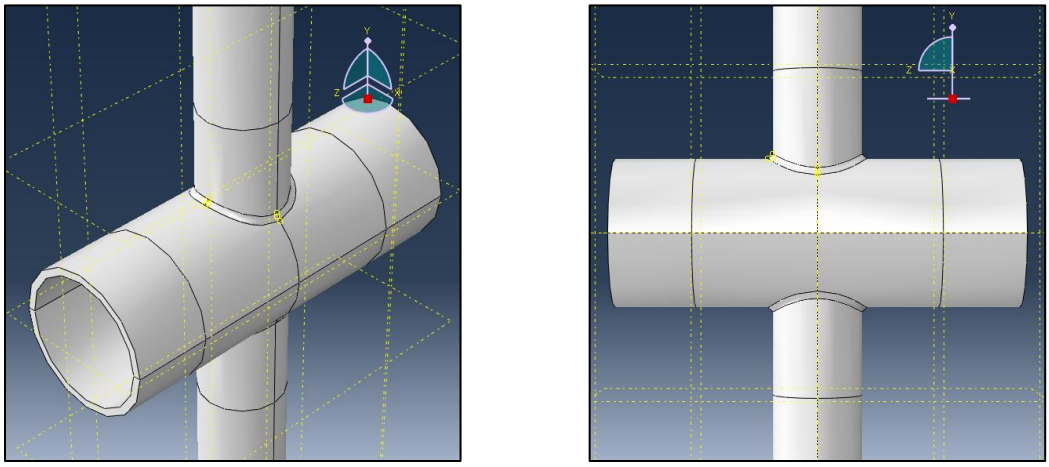


Figure 5. *Baseline model of the fillet-welded joint, as modelled in Abaqus.*

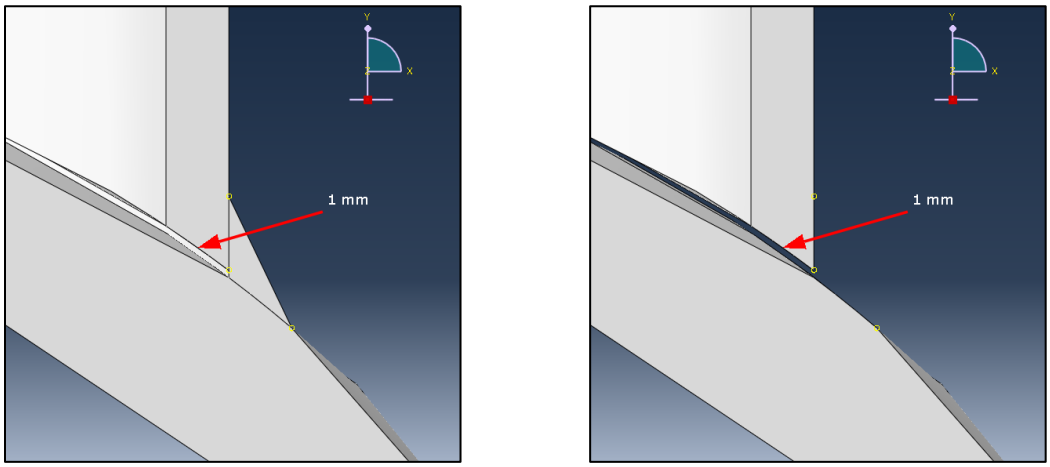


Figure 6. *Fillet weld root gap, as modelled in Abaqus. Left: cross-section view at the saddle of the joint; right: fillet weld hidden, highlighting the root gap.*

The models were partitioned into several regions with varying mesh sizes. A finer mesh was applied to the regions close to the connection. For the area further away, a coarser mesh was used. This was done to lower the computational demands. Specifically, a mesh size of 3 mm was applied to the area within 300 mm in the length of the chord and 400 mm in the length of the brace, measured from the centre of the joint. The applied mesh size for the outer regions is 7 mm.

For the models with T = 46 mm, the mesh size for the area near the connection was set to 4 mm to limit the number of mesh elements. This was necessary because a high thickness of the chord causes a steep increase in the number of mesh elements. Slightly increasing the mesh size brought down the computation time and significantly reduced the amount of physical memory needed to run the analysis.

As a result of the varying model dimensions, the total number of elements ranges from approximately 500,000 (for T = 9.2 mm) to roughly 1,400,000 elements (for T = 30.7 mm). The models with T = 46 mm contain around 700,000 elements due to the adjusted mesh size. Figure 7 illustrates the meshed fillet-welded model for T = 20 mm.

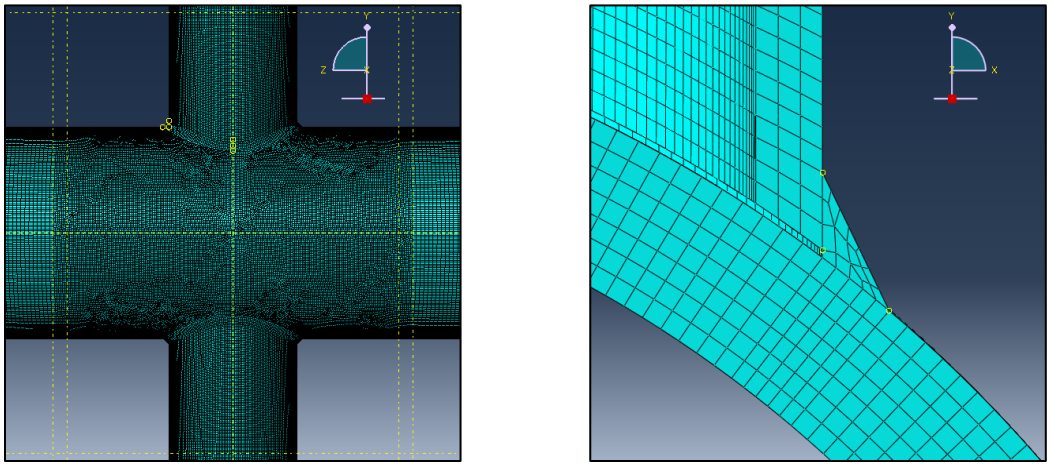


Figure 7. *Meshed fillet-welded model for T = 20 mm. Left: overview of the meshed model; right: detailed view of the meshed fillet weld.*

3.2 Parametric Study

The parametric study was performed using a similar method as highlighted in Cao et al. (2018); Kumar et al. (2018). Unlike their studies, this study focused solely on the influence of the brace-to-chord thickness ratio τ and the chord slenderness ratio γ. As described in Section 3.1, this was done by varying T while keeping the other joint dimensions constant. The choice of the baseline model dimensions, as previously listed in Table 1 in Section 3.1, was supported by the parametric DNV study presented in Section 2.3. This theoretical parametric study showed that the SCFs reach their maximum at a diameter ratio β of approximately 0.6 and at an angle θ between the chord and brace of 90 degrees. Thus, the baseline model represents the most critical case.

The value of γ was incrementally varied by changing T accordingly, this increases the value of τ as well. Table 3 lists all the used model variations.

Table 3
Model variations used for the parametric study

γ	T	$D/T \leq 40^a$	τ
4	46.0	8.0	0.19
6	30.7	12.0	0.29
8	23.0	16.0	0.38
9.2[b]	20.0	18.4	0.44
10	18.4	20.0	0.48
12	15.3	24.0	0.57
14	13.1	28.0	0.67
16	11.5	32.0	0.77
18	10.2	36.0	0.86
20	9.2	40.0	0.96

Note. The values shown in red fall outside the range of validity given in DNV-RP-C203 (DNV, 2021).
[a] According to NEN-EN 1993-1-8 (NEN, 2025b), the ratio between the chord diameter and thickness needs to stay below a value of 40 for welded X-joints between CHS brace members and chords.
[b] The baseline model, as drawn from Schürmann et al. (2020).

3.3 SCF Calculation Using the Hot-Spot Stress Method

Linear extrapolation was used to determine the hot-spot stresses. At points *a* and *b* from the weld toe, the maximum principal stresses were extracted from Abaqus. DNV-RP-C203 (DNV, 2021) proposes to determine the values of *a* and *b* using the equations provided in Table 4. Figure 8 illustrates a general welded joint and defines the corresponding parameters and extrapolation points.

Table 4
Extrapolation points, as proposed in DNV-RP-C203 (DNV, 2021)

Point	Chord saddle	Chord crown	Brace saddle	Brace crown
a	$0.2\sqrt{rt}$	$0.2\sqrt{rt}$	$0.2\sqrt{rt}$	$0.2\sqrt{rt}$
b	$\frac{\pi R}{36}$	$0.4\sqrt[4]{rtRT}$	$0.65\sqrt{rt}$	$0.65\sqrt{rt}$

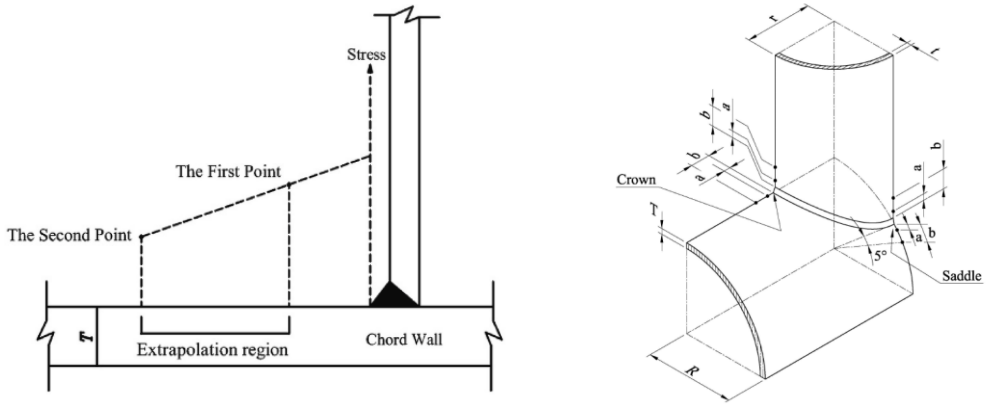


Figure 8. *Left: extrapolation points (Zavvar et al., 2025); right: geometric parameters DNV-RP-C203 (DNV, 2021).*

Since these locations did not directly coincide with the mesh, the stress values at these points were obtained by linearly interpolating the values of the neighbouring mesh nodes along the selected path. Subsequently, these values were extrapolated to the location of the weld toe. Using this method, the hot-spot stresses σ_{HS} were determined for each model at the chord saddle, chord crown, brace saddle, and brace crown.

The nominal stress σ_{nom} in the brace was calculated using the equation from Section 2.1. With t = 8.8 mm and d = 220.8 mm (A = 5,860.96 mm^2), and an applied force of 500,000 N, this stress equals 85.31 MPa. By dividing the obtained hot-spot stresses by this value, the SCFs were determined.

4 Results

With the 20 models, a total of 80 SCF values were determined. This provides insight into how the SCFs are influenced by the type of weld, the location in the joint, and the thickness of the chord.

Table 5 shows the stress concentration factors for the butt-welded joint. These are shown in a line plot against the chord slenderness γ. From the graph in Figure 9, it can be deduced that for an increasing γ (and therefore also an increasing τ), the SCF increases at the saddle of the joint in both the brace members and chord. At the location of the crown, the stress concentration decreases to almost zero. The most critical point is at the saddle point, specifically in the chord. For a decreasing chord thickness T, the SCF becomes considerably higher here.

Table 5
Stress concentration factors for the butt-welded joint

γ	τ	SCF			
		Chord		Brace	
		Saddle	Crown	Saddle	Crown
4	0.19	0.95	0.65	1.17	0.83
6	0.29	2.24	1.03	2.92	1.39
8	0.38	3.94	1.14	4.50	1.34
9.2	0.44	5.42	1.15	5.59	1.28
10	0.48	7.39	1.10	6.40	1.21
12	0.57	9.55	0.96	8.60	0.99
14	0.67	14.79	0.61	11.08	0.60
16	0.77	17.13	0.36	13.47	0.33
18	0.86	24.63	0.27	16.44	0.24
20	0.96	31.06	-0.09	18.98	0.02

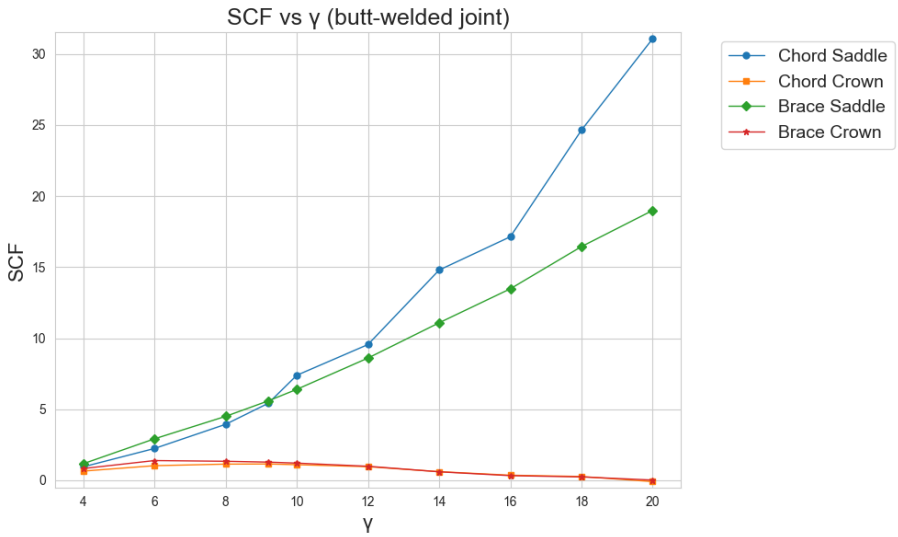


Figure 9. *Plot of the stress concentration factors against the chord slenderness γ, for the butt-welded joint*

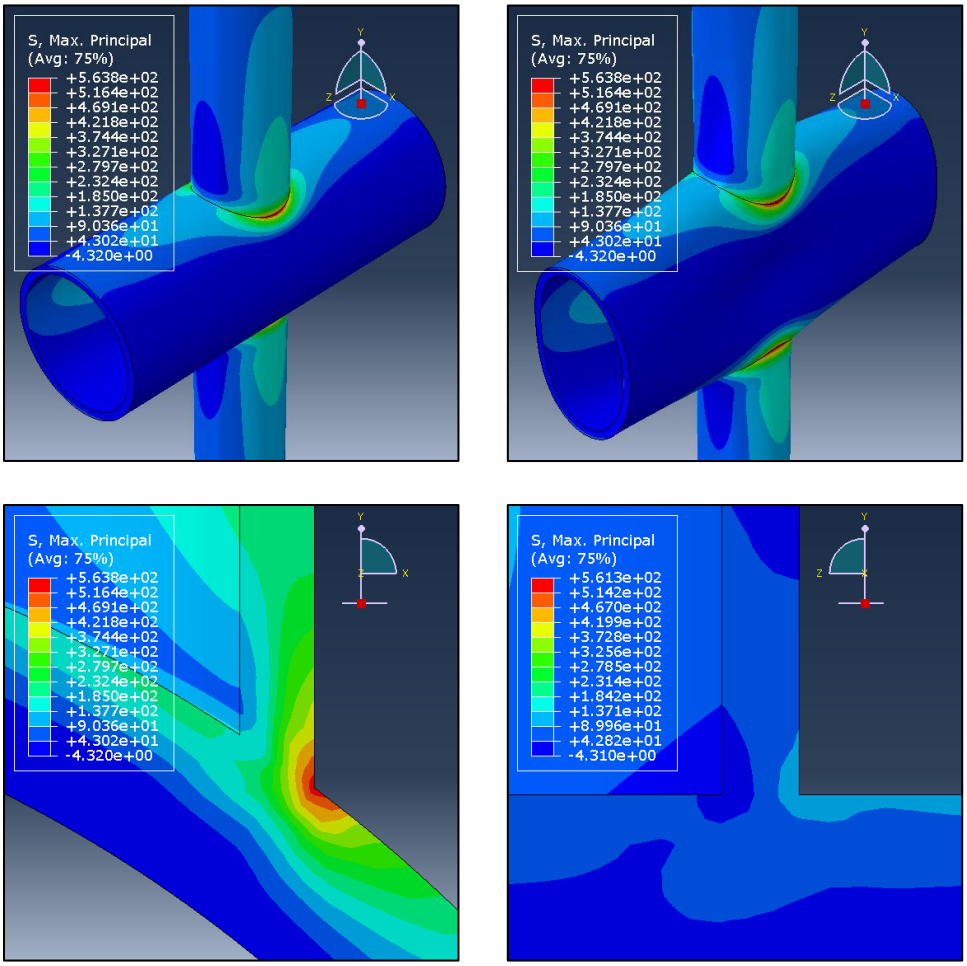


Figure 10. *Maximum principal stresses in the butt-welded joint with baseline geometry. Upper left: stresses masked on the undeformed model; upper right: stresses masked on the deformed model; bottom left: stresses in the connection at the saddle; bottom right: stresses in the connection at the crown.*

To provide an idea of the stress distribution in the butt-welded joint, the Abaqus output for one model is shown in Figure 10. The most stress is built up in the saddle region. At the crown there is hardly any stress build-up. These observations correspond with the calculated SCF values.

In Table 6 the stress concentration factors are given for the fillet-welded joint. These are also shown in a line plot against the chord slenderness γ. The graph in Figure 11 shows similar results as Figure 9. Here too the SCF increases as γ and τ become larger. It is remarkable that here the values of the SCFs are lower than in the butt-welded model. For this type of connection there is almost no stress concentration in the crown either and the saddle is the most affected region. It is noticeable that in this case, for a low value of γ (large thickness T) the stress mainly accumulates in the brace, and only from approximately γ = 14 becomes governing in the chord saddle. The build-up of stresses in the brace members is very clearly visible in Figure 12.

Table 6
Stress concentration factors for the fillet-welded joint

γ	τ	SCF			
		Chord		Brace	
		Saddle	Crown	Saddle	Crown
4	0.19	0.90	0.55	2.60	1.75
6	0.29	1.63	1.00	3.84	1.24
8	0.38	2.92	1.20	5.13	1.08
9.2	0.44	5.42	1.15	5.59	1.28
10	0.48	4.76	1.22	6.51	0.84
12	0.57	7.11	1.16	8.03	0.48
14	0.67	9.95	1.01	9.59	0.09
16	0.77	13.42	0.86	11.01	0.00
18	0.86	17.04	0.53	12.76	0.00
20	0.96	21.55	0.19	14.25	0.01

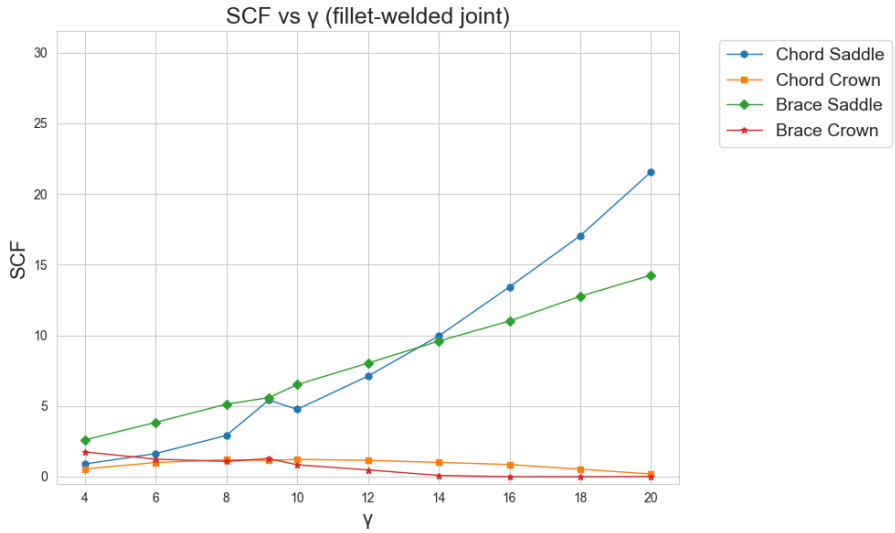


Figure 11. *Plot of the stress concentration factors against the chord slenderness γ, for the fillet-welded joint*

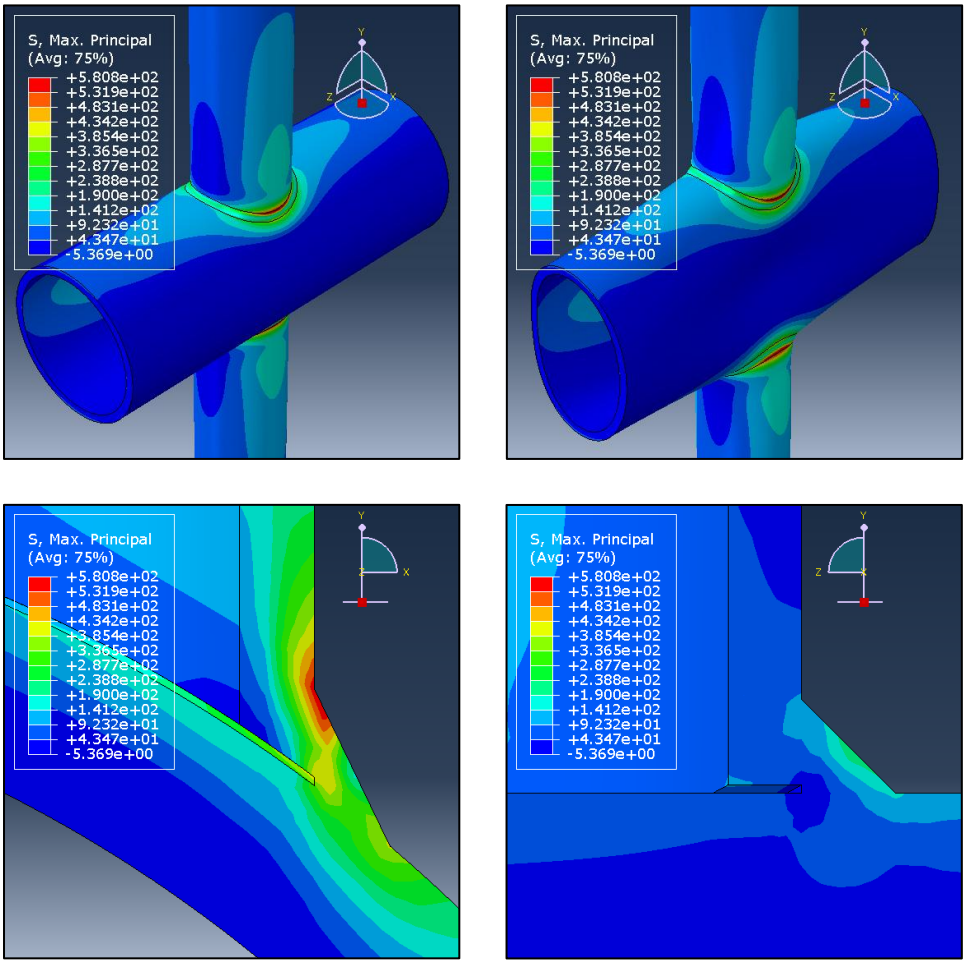


Figure 12. *Maximum principal stresses in the fillet-welded joint with baseline geometry. Upper left: stresses masked on the undeformed model; upper right: stresses masked on the deformed model; bottom left: stresses in the connection at the saddle; bottom right: stresses in the connection at the crown.*

5 Discussion

This research was conducted to investigate how the geometry and type of weld of a joint influence the stress concentration factor. This was done using Abaqus by performing a stress analysis on multiple models, each with a different chord wall thickness. This was done for a butt-welded joint and for a joint connected with a fillet weld with a weld length of 11.3 mm.

The results obtained in Section 4 show that with increasing chord slenderness γ and brace-to-chord thickness ratio τ, the SCF increases. This means that: the thinner the chord wall relative to the chord diameter D and brace wall thickness t, the higher the SCF. The strongest effect is observed at the saddle region.

It is noticeable that for a joint with fillet welds, the SCF values are much lower than for a joint with butt welds. This is clearly shown in Figure 13. For example, the maximum SCF found for the butt-welded joint is 31.06 and for the fillet-welded joint it is equal to 21.55. That is approximately a 30.6% reduction by adding a fillet weld.

Even though a sizeable discontinuity was introduced in the fillet weld by leaving a 1 mm gap between the chord and the brace members, it still is better to use than a butt weld. A fillet weld adds material, where a butt weld replaces material. Adding extra material ensures that the stresses, which have a larger and more gradual transition area, can 'flow' better between brace member and chord.

For a butt-welded joint with a chord wall thickness T of 13.1 mm, an SCF of 14.79 occurs in the chord saddle. For a fillet-welded joint with a T of 11.5 mm, an SCF of 13.42 occurs in the chord saddle. A lower SCF, but with a 1.6 mm thinner chord. Now imagine that a 1.6 mm thinner cross-section is used over an entire chord of 1000 mm long, then more than 1,726,116 mm3 (13.55 kg) of steel can be saved. This is much more material than is needed to create a fillet weld. It therefore has both economic and ecological advantages to use fillet welds. Only with a low chord slenderness ($\gamma \leq 10$) and therefore large wall thickness, the SCF becomes higher than in a model with a butt-weld. This happens in the brace saddle.

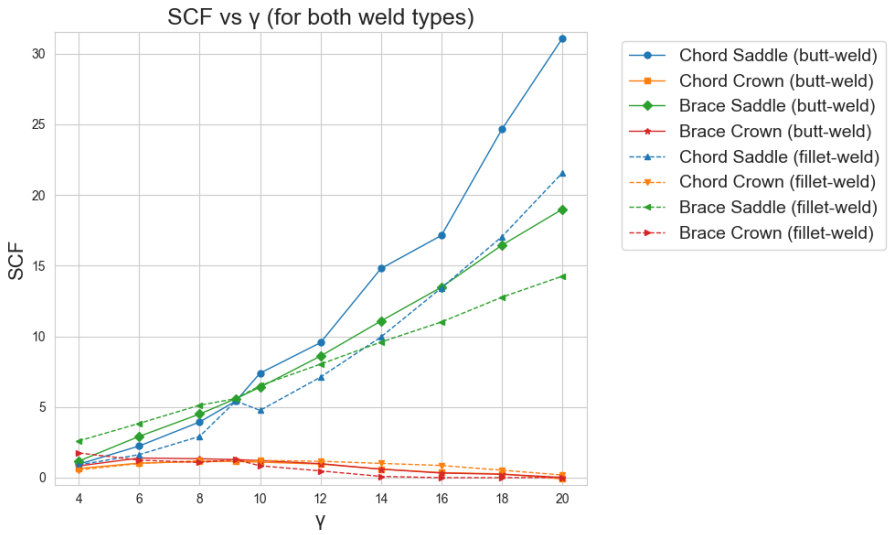


Figure 13. *Comparison between the SCFs of the butt- and fillet-welded joint*

In order to validate the results of this research, the outcomes were compared with the empirical formulas for the SCFs as given in DNV-RP-C203 (DNV, 2021), see Section 2.3. The differences can easily be displayed by means of a graph, which can be seen in Figure 14. At a glance it can be seen that the results are reasonably similar. Especially for the saddle SCFs of the butt-welded joint.

The empirical equations of the DNV seem to overestimate the stresses at the crown position, however. The brace crown SCFs do show the same slightly decreasing behaviour, but the values are predicted too high compared to the FEA results. The values at the chord crown do not match well. These slight differences could be caused by the fact that design guides usually work with more conservative values.

The large difference in the values for the chord saddle, between the DNV and the fillet-welded joint from this study, shows that the DNV is not applicable everywhere. The values predicted by the DNV are many times larger than the actual value for a high chord slenderness. The DNV does not take the dimensions and type of the weld into account in its empirical formulas. The differences clearly show how important it is to make an accurate model and to continue expanding the design guides for more different cases. Two models were also made for the fillet and butt-welded joint that are outside the DNV range of validity ($\gamma = 4$ and $\gamma = 6$) to see to what extent the DNV rules still apply. That did not lead to any extraordinary results.

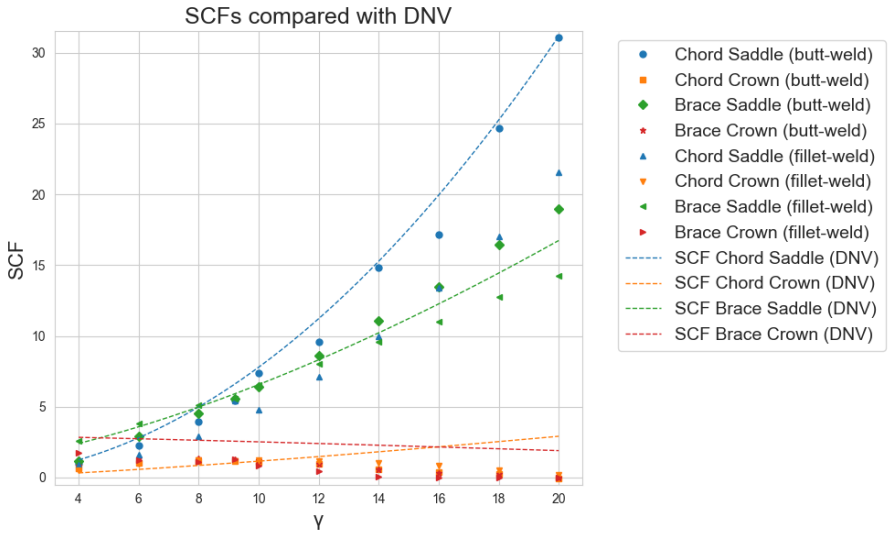


Figure 14. *Comparison between the SCFs as found in this research, and as formulated in the DNV guidelines.*

This research had a number of limitations. Namely, it focused entirely on 90° X-joints with circular hollow sections. In Section 2.3 it was found that this angle led to the highest stress concentration in the joint and considering the short time in which this research had to be performed, the number of different models was kept as limited as possible. The research is not applicable to other types of connections, such as Y- or K-joints, or non-circular sections. In contrast to studies such as Cao et al. (2018), only static axial loading was taken into account as well, excluding bending moments or dynamic loads.

To simulate the behaviour of a poorly applied fillet weld, a gap of 1 mm between the chord and brace members was introduced. This could have caused the SCFs to be estimated higher or lower than in real-world scenarios. In reality, welds often differ in quality and there could be a larger or smaller gap, or no root gap at all.

6 Conclusions and Recommendations

The aim of this study was to answer the following main research question:

> How do the geometric parameters and weld type of a tubular X-joint influence the stress concentration factors?

Based on the results of the finite element analysis, it can be concluded that both the chord slenderness ratio γ and brace-to-chord thickness ratio τ have a significant influence on the stress concentration factors (SCF). Increasing these ratios by decreasing the chord thickness T leads to an increase in the SCFs, especially in the saddle region of the joint. The smaller the difference between T and the brace thickness t, the higher the local stress peaks.

The type of weld also clearly influences the values of the SCFs. A model with fillet welds consistently shows lower SCF values than a model with butt welds. Although a root gap of 1 mm was introduced between the chord and brace members to simulate an imperfect weld, the fillet welds still yielded lower SCF values. This is due to the amount of added material at the location of the connection, which ensures that the stresses in the brace members and chord can flow more smoothly.

The maximum SCF for the butt-welded joints is 31.06. For the fillet-welded joints a maximum SCF of 21.55 was found. These maxima are around the chord saddle. Adding a fillet weld can lead to a SCF reduction of approximately 30.6%. For lower chord slenderness ratios than fourteen, the dominant SCF for the fillet-welded joint shifted from the chord to the brace saddle.

These findings demonstrate that fillet welds are not only structurally advantageous, but also economically and ecologically beneficial, as they allow for a thinner chord thickness. Thus, saving material, without compromising structural safety and resistance.

The results closely matched the empirical formulas from DNV-RP-C203 for butt-welded joints but showed larger deviations for fillet welds – particularly at the chord saddle. This underlines that existing design guidelines do not sufficiently consider the type and geometry of the weld and supports the need for further model-based research.

This research was limited to X-joints connected under 90 degrees with circular hollow sections (CHS), and due to the short time in which this research was performed the number of models was limited to 20. The welds were simplified somewhat, by assuming a constant root gap of 1 mm. In reality the weld quality will vary, and gaps may be larger or smaller.

For future research, it is recommended to expand the number of models with fillet-welded joints, without root gap, and with a larger root gap. In this way, variations in weld quality can be simulated and analysed. Also, varying the weld size would create valuable additional insight into how weld geometry affects SCFs.

Another recommendation is to investigate different joint angles. In this way, even more parameters can be investigated for their effect on SCFs.

With an increased number of models, it may also become feasible to derive empirical formulas for SCFs at various regions of the joint, based on the finite element results. Overall, this study contributes new insights into the behaviour of welded X-joints under axial loads and demonstrates how optimized weld detailing can enable more material-efficient structural designs.

References

Ahmadi, H., Lotfollahi-Yaghin, M. A., Yong-Bo, S., & Aminfar, M. H. (2012). Parametric study and formulation of outer-brace geometric stress concentration factors in internally ring-stiffened tubular KT-joints of offshore structures. *Applied Ocean Research*, *38*, 74-91. https://doi.org/10.1016/j.apor.2012.07.004

Cao, Y. G., Zhen, Y., Liu, C., Zhang, S. H., & Meng, Z. B. (2018). Parametric Study of Stress Concentration Factors (SCFs) on Tubular X-Joints Used in Offshore Platform Structures. *Journal of Coastal Research*, *34*(4), 987-995. https://doi.org/10.2112/jcoastres-d-17-00132.1

DNV. (2021). *Fatigue design of offshore steel structures* (Recommended Practice No. C203). https://standards.dnv.com/explorer/document/97A75DD254F44200BE218CF21FE5B504/8

Kumar, L., Kumar, A., Barnat-Hunek, D., Szczygielska, E., & Garbacz, M. (2018, Nov 22-24). SCFs study of tubular T/Y steel joints under inplane loading. *MATEC Web of Conferences* [Iii international conference of computational methods in engineering science (cmes 18)]. 3rd International Conference of Computational Methods in Engineering Science (CMES), Kazimierz Dolny, Poland https://doi.org/10.1051/matecconf/201925206010

NEN. (2019). *Eurocode 1: Actions on structures – Part 1-1: General actions – Densities, self-weight, imposed loads for buildings* (Norm No. NEN-EN 1991-1-1+C1+C11). https://www.nen.nl/nen-en-1991-1-1-c1-c11-2019-nl-207218

NEN. (2025a). *Eurocode 3 - Design of steel structures - Part 1-1: General rules and rules for buildings* (Norm No. NEN-EN 1993-1-1). https://www.nen.nl/nen-en-1993-1-1-2025-en-303760

NEN. (2025b). *Eurocode 3 - Design of steel structures - Part 1-8: Joints* (Norm No. NEN-EN 1993-1-8). https://www.nen.nl/nen-en-1993-1-8-2025-en-322620

Schürmann, K., Schaumann, P., Pittner, A., & Rethmeier, M. (2020). Experimental investigations on the fatigue resistance of automatically welded tubular X-joints for jacket support structures. *Journal of Physics: Conference Series*, *1669*(1), 012022. https://doi.org/10.1088/1742-6596/1669/1/012022

Zavvar, E., Rosa-Santos, P., Ghafoori, E., & Taveira-Pinto, F. (2025). Analysis of tubular joints in marine structures: A comprehensive review. *Marine Structures*, *99*, Article 103702. https://doi.org/https://doi.org/10.1016/j.marstruc.2024.103702

Author's Note: Parts of this thesis have been rewritten with the help of OpenAI's GPT-3.5 model. It was exclusively used to improve clarity and to rewrite Dutch to English. No factual or analytical content was generated. See: https://openai.com/about/

